SUPPORTING INFORMATION APPENDIX

STED nanoscopy of the centrosome linker reveals a CEP68-organised, periodic rootletin network anchored to a C-Nap1 ring at centrioles

Rifka Vlijm[1,2,9], Xue Li[3,7,9], Marko Panic[3,7], Diana Rüthnick[3], Shoji Hata[3], Frank Herrmannsdörfer[4], Thomas Kuner[4], Mike Heilemann[4,5,6], Johann Engelhardt[1,2], Stefan W. Hell[1,2,8] and Elmar Schiebel[3]

[1] German Cancer Research (DKFZ), Im Neuenheimer Feld 280, 69120 Heidelberg, Germany
[2] Max Planck Institute for Medical Research, Department of Optical Nanoscopy, Jahnstr. 29, 69120 Heidelberg, Germany
[3] Zentrum für Molekulare Biologie der Universität Heidelberg (ZMBH), Deutsches Krebsforschungszentrum (DKFZ)–ZMBH Allianz, Universität Heidelberg, 69120 Heidelberg, Germany
[4] Department of Functional Neuroanatomy, Institute for Anatomy and Cell Biology, Universität Heidelberg, 69120 Heidelberg, Germany
[5] BioQuant, Im Neuenheimer Feld 267, Universität Heidelberg, 69120 Heidelberg, Germany
[6] Institute of Physical and Theoretical Chemistry, Johann Wolfgang Goethe-University, 60438 Frankfurt, Germany
[7] Hartmut Hoffmann-Berling International Graduate School of Molecular and Cellular Biology (HBIGS), Universität Heidelberg, 69120 Heidelberg, Germany
[8] Max Planck Institute for Biophysical Chemistry, Department of NanoBiophotonics, Am Fassberg 11, 37077 Göttingen, Germany
[9] both authors contributed equally

Contents

Details of Materials and Methods

STORM. (1) 3D-STORM was performed as described previously on a custom-built setup (2). In brief, a 660 nm and a 405 nm laser (Cube; Coherent) were focused into the back focal plane of the 100×/1.49-NA (numerical aperture) oil immersion objective lens (Olympus). Excitation and fluorescence emission were separated using appropriate filters (Chroma, Bellow Falls), and single-molecule fluorescence was recorded with an EMCCD camera (iXon Ultra 897; Andor) operated in the continuous imaging mode. In order to generate the 3-dimensional information a cylindrical lens with a focal length of 1000 mm (Thorlabs) was integrated in the emission path. MicroManager (3) was used to acquire the images and the z-focus was stabilised via a piezo-based objective positioner (Physik-Instrumente). To induce photoswitching of the Alexa Fluor 647 dye we used high laser intensity of the 660 nm laser (~2 kW/cm^2) and a 405 nm laser was used in order to increase the transition rate between the dark and emitting state. Typically, 40,000 frames were recorded with an exposure time of 30 ms. For single-molecule localisation and reconstruction rapidSTORM (4) was used followed by a bead-based drift-correction with a custom-written Java script. The images were further analysed using the open source software ViSP (5). The samples were kept in a 100 mM MEA buffer for the imaging process.

Cell Culture and Transfection. Non-transformed human telomerase-immortalised retinal pigmented epithelial cells (RPE-1) cells were maintained in Gibco DMEM/F-12 (ThermoFisher). HCT116 cell lines were cultured in McCoy's 5A (modified) medium, GlutaMAX supplement (ThermoFisher). Both media were supplemented with 10% FBS, 1 % L-glutamine and 1 % penicillin/streptomycin. HUVEC cells were cultivated in the Endopan 3 endothelial cell kit (PanBiotech) supplemented with 1 % penicillin/streptomycin. All cell lines were grown at 37°C with 5% CO2. For siRNA transfection, Lipofectamine RNAiMAX (ThermoFisher) was used according to the manufacturer's instructions with a final concentration of 20 nM siRNA. The following siRNA oligos were used: Non targeting siRNA (non-specific control (NSC), Human Dharmacon ON-Target plus, Nr. 1, Thermo Scientific, sequence: 5´-UGUUUACAUGUCGACUAA-3´), rootletin siRNA (Ambion by Life Technologies, 216869, sequence: 5'-GCAUGUGUCGGGAAAUUCCtt-3'), CEP68 siRNA (Ambion by Life Technologies, 136783, sequence: 5'-GCACCUUGAUAGCCGUGUGUU-3'), C-Nap1 siRNA (Human CEP250 Dharmacon ON-TARGET plus, No. 1 and 3, Thermo Scientific, sequence: 5'-GAGCAGAGCUACAGCGAAU-3' and 5´-AAGCUGACGUGGUGAAUAA-3). For plasmid transfection, Lipofectamine LTX (ThermoFisher) was used according to the manufacturer's instructions.

Generation of stable cell lines. The tetON system was used to control protein expression. RPE-1 tetR cell line was generated according to the manufacturer's protocol (Retro-X Tet-On 3G Inducible Expression System User Manual, Clontech Laboratories, Inc) with blasticidin selection. This hTERT-RPE-1 tetR cell line was used as control cell line in this paper. In order to generate Dox-inducible stable cell lines, retroviral-mediated integration was used. For production of viral particles, the gene of interest was cloned into pRetroX-TRE3G (Clontech) and co-transfected with the envelope vector pCMV-VSV-G (Addgene) to a HEK293-based retroviral packaging cell line (GP2-293, Clontech). Media was changed after 24 h and after 48

h the virus containing media was harvested and filtered using a 0.45 µM filter (Millipore). Four parts of filtered virus medium were supplemented with two parts fresh media, one part FBS and 4 µg/ml Polybrene (Sigma). RPE-1-tetR cells pre-seeded in a 6-well plate were infected by adding the virus-containing solution three times every 4 – 6 h. Cells were split 24 h after the first transduction and put under puromycin selection after 48 h. In overexpression experiments, stable cell lines were seeded on glass coverslips overnight with around 20% confluence, doxycycline (+Dox) induction was performed with 20 ng/ml final concentration for 24 h. Rootletin was cloned from pEGFP-rootletin plasmid (A kind gift from Dr. Andrew Fry, University of Leicester). pcDNA3-FLAG-CEP68 plasmid was from Dr. Michele Pagano from New York University. There was leaky *CROCC* (rootletin) expression in RPE-1 tetON rootletin-HA cell line without doxycycline induction (Fig. S8*H and I*). This mild *CROCC* (rootletin) overexpression condition was used in the experiments with the RPE-1 tetON rootletin-HA cell line. The rootletin fragments are: R1 (aa 1-494), R2 (aa 495-1078), R3 (aa 1079-1825), R4 (aa 1826-2017), R123 (aa 1-1825) and R234 (aa 495-2017).

Immunofluorescence. For indirect immunofluorescence, cells were seeded on a coverslip, washed once with PBS and fixed with ice-cold methanol for 5 min at -20°C. The sample was permeabilised with 0.1% Triton X-100 for 10 min, unspecific binding was blocked with 10% (v/v) FBS for 30 min followed by incubation in the primary antibodies in 3% (w/v) BSA for 1 h in a humid chamber. After three consecutive washing steps with PBS, the sample was incubated with the secondary antibody in 3% BSA for 30 minutes. DNA was co-stained with DAPI. The coverslip was mounted on a glass slide with Mowiol (Calbiochem) with and without PPD (Sigma).

Antibodies. The following primary antibodies were used in immunofluorescence microscopy experiments: rabbit anti-rootletin (polyclonal antibody, antigen rootletin aa 1826-2017; root-C1; 1:100) (6), mouse anti-rootletin (monoclonal antibody, antigen rootletin aa 1882-1917, root-C2; Santa Cruz, sc-374056; 1:100), rabbit anti-rootletin (polyclonal antibody, antigen rootletin aa 1-494, root-N; 1:100) (6), rabbit anti-Cep68 (polyclonal antibody, antigen CEP68 aa 1-497; 1:800) (7), goat anti-C-Nap1 (1:800) (6), mouse anti-C-Nap1 (antigen C-Nap1 aa 1988-2442; 1:2) (8), mouse anti-γ-tubulin (Abcam, ab27074; 1:10000), guinea pig anti-pericentrin (PCNT) (1:500), mouse anti-GT335 (AdipoGen, AG-20B-0020; 1:500) (9), mouse anti-CENP-F (anti-Mitosin; BD Biosciences, 610768; 1:100), rat anti-HA (Roche, 3F10; 1:500). The following secondary antibodies were used in immunofluorescence microscopy experiments: donkey anti-rabbit IgG coupled to Alexa Fluor 488, Alexa Fluor 555 or Alexa Fluor 647, donkey anti-mouse IgG coupled to Alexa Fluor 488, Alexa Fluor 555 or Alexa Fluor 647, donkey anti-goat IgG coupled to Alexa Fluor 488, anti-mouse IgG coupled to Alexa Fluor 488, Alexa Fluor 555 or Alexa Fluor 647, goat anti-guinea pig IgG coupled to Alexa Fluor 555 or Alexa Fluor 647, donkey anti-rat IgG coupled to Alexa Fluor 488 (Invitrogen; all 1:500). Donkey anti-guinea pig IgG coupled to CF 488 (Sigma; 1:500). The following primary antibodies were used in western blot experiments: rabbit anti-rootletin (root-C1; 1:100) (6), rabbit anti-Cep68 (1:500) (7), mouse anti C-Nap1 (BD Biosciences, 611375; 1:500), rat anti-HA (Roche, 3F10; 1:1000) and rabbit anti-GAPDH (Cell Signaling Technology, 2118; 1:5000). The following secondary antibodies were used in western blot experiments: HRP (horseradish peroxidase)-conjugated donkey anti-rabbit IgG (H+L), HRP-conjugated donkey anti-rat IgG (H+L), HRP-conjugated goat anti-mouse IgG+IgM (H+L) (Jackson; 1:5000) HRP-conjugated donkey anti-guinea pig IgG (H+L) (Dianova, 706-035-148; 1:5000).

Sample preparation for western blots. Cells were washed with PBS. Cells were lysed in Laemmli Buffer plus Benzonase (Merck, 101656; 1:500) on ice for 15 min. The lysates were collected by scrapers and transferred into 1.5 ml tubes. Lysates were cleared by centrifugation (14,000 for 15 min at 4°C) and heated at 95°C for 5 min.

Live cell imaging. Live cell imaging was performed using DeltaVision RT system at 37°C. Doxycycline-inducible RPE-1 cell line expressing mNeonGreen-CEP68-P2A-mRuby2-PACT (RPE-1 FRT/T-Rex mNeonGreen-CEP68-P2A-mRuby2-PACT) was generated using the FLIP-in system (Flp-In T-Rex RPE1 cells, a kind gift from Dr. Jonathon Pines, The Gurdon Institute) and a modified pcDNA5/FRT/TO vector (Invitrogen). This cell line was used in live cell imaging. 2 ng/ml Dox was used for induction of expression. Cells were imaged in DMEM/F12 (HEPES, no phenol red, with all supplements; ThermoFischer) in Ibidi µ-Slide 8 well (Ibidi). Cells were imaged every 30s for a 1 hour with total 121 frames. Images were processed with deconvolution and projection with max intensity.

Supplemental Figures

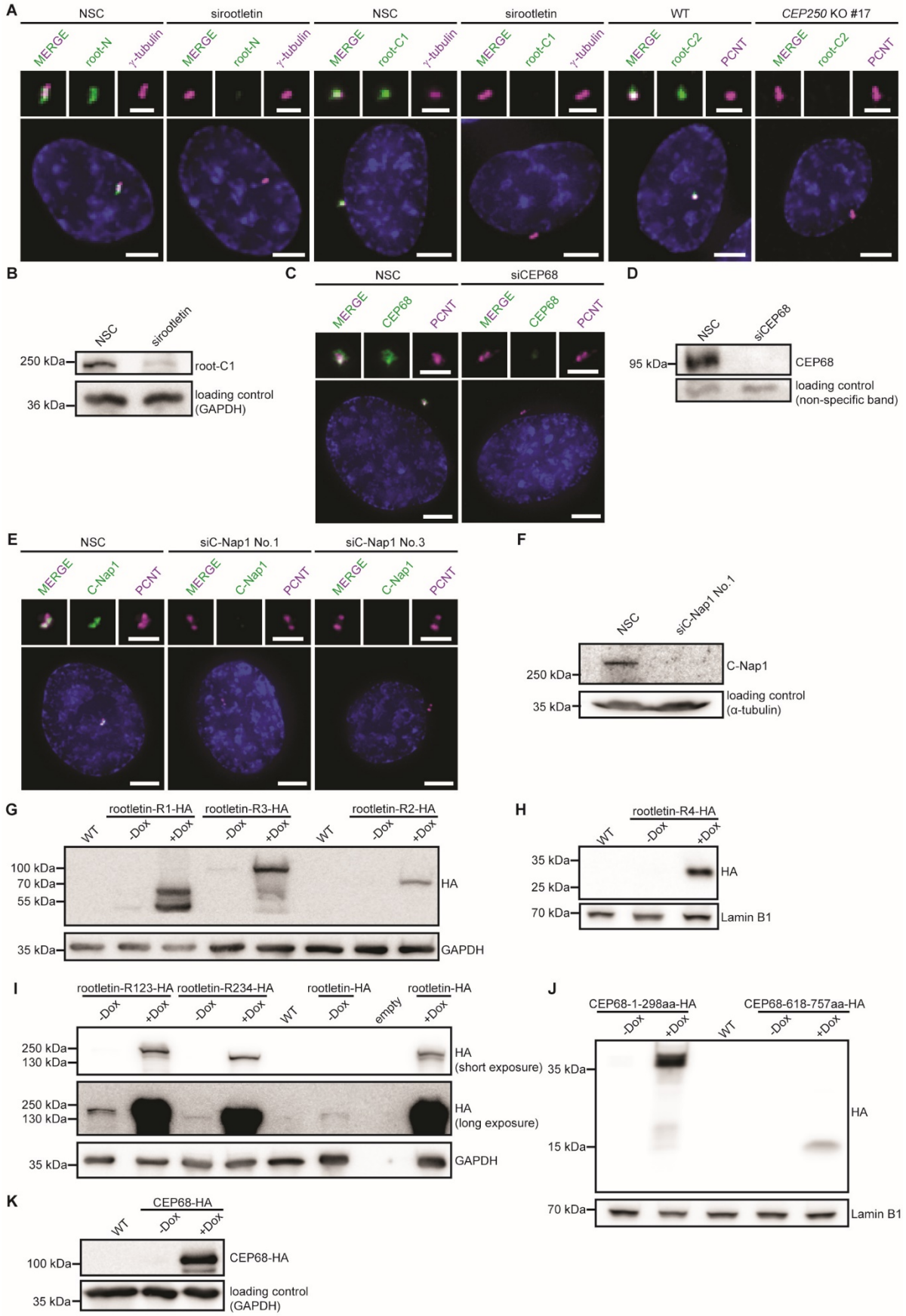

Supplemental Fig. 1. Confirmation of the specificity of siRNAs, antibodies and overexpression by tetON systems used in this study. (A, B) Confirmation of the specificity of different rootletin antibodies (root-N, root-C1, and root-C2) by indirect immunofluorescence (IF) (A) and root-C1 by immunoblotting (B). (C, D) Confirmation of CEP68 depletion and the specificity of CEP68 antibody by IF and immunoblotting. (E, F) Confirmation of C-Nap1 depletion and the specificity of C-Nap1 antibody by IF and immunoblotting. (G-I) Confirmation of Dox induced overexpression of rootletin-HA, rootletin-R1-HA, rootletin-R2-HA, rootletin-R3-HA, rootletin-R4-HA, rootletin-R123-HA, rootletin-R234-HA in TetON system by immunoblotting. Note the leaky expression of rootletin constructs without addition of Dox. (J, K) Confirmation of Dox induced overexpression of CEP68-1-298aa-HA, CEP68-618-757aa-HA, and CEP68-HA in tetON system by immunoblotting. Scale bar: 5 µm in whole cell images and 2.5 µm in enlarged images.

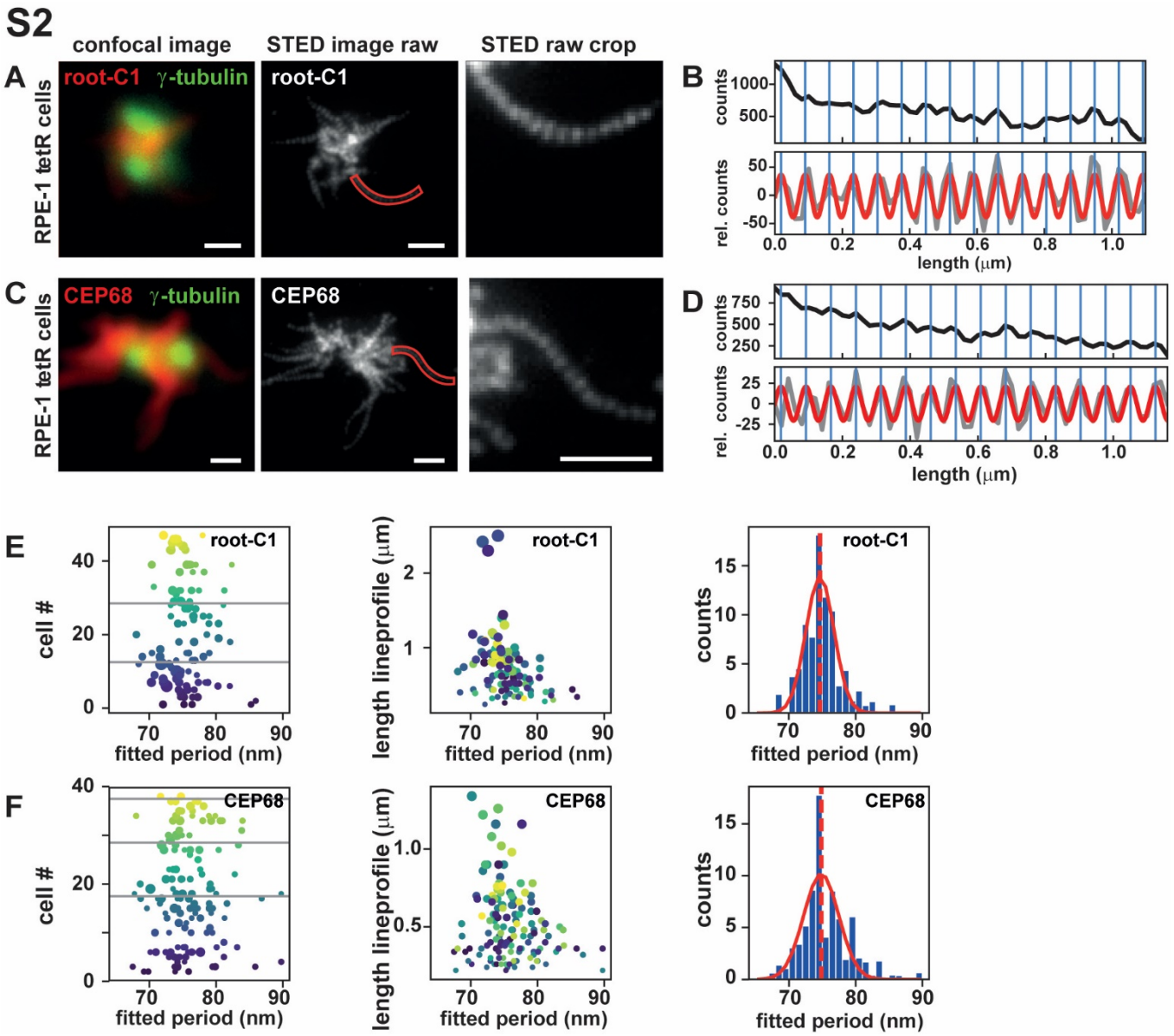

Supplemental Fig. 2. Method of periodicity fitting. (A-D) For objectivity, the periodicity of the rootletin and CEP68 fibres are determined through an automated fitting procedure as follows: First, a confocal image is made of either rootletin (root-C1, A) or CEP68 (B) in combination with γ-tubulin to determine the centrosome location (left panels). Next, a STED-image of rootletin (A) or CEP68 (B) is made (middle panels). Of each filament that is in focus, the path is determined (examples are marked red in right middle panels A and C, for clarity, a zoom of the example filaments is shown in the right panels, all scaled from minimal to maximal measured intensities) and an intensity line profile is made from a few pixel wide line along the filament in the raw STED image (B and D) using ImageJ. To obtain clear locations of the peaks, the moving average of the intensity (window size = 3 pixels, e.g. 60 nm) was subtracted from the line-profile (resulting in the grey curves in B and C). At this point a sine-function was fitted to the obtained peaks (red curves in B and D). Each fitted sine-function was manually checked for correctness by looking at the fitted peak locations (blue lines in B and D) compared to the raw-data line profile (black line B and D). It turned out that many line profiles (35 of the 147) were difficult to fit to a sine-function. In most cases a significant part shows a periodicity close to 75 nm, however breaks along the length of the filament shift the phase such that it is not possible to fit a single sine function along the entire length of the filament. Examples of these events are indicated by the red arrows in Fig. 1B. If these line profiles

were to be cut up, similar results would come out of those sine-fits, compared to the line-profiles that were well fitted from the beginning. (E) The results of 112 line-profiles from rootletin fibres with a total length of 79.48 nm (~1060 periods), from three individually prepared samples that could be fitted using an automated procedure. In the left two panels, the fitted periodicity of each filament is plotted as an individual dot, each cell has its own colour and the size of the spot represents the filament length. Left: the fitted periodicity as a function of the cell number indicates that each cell gives a similar result. The grey lines indicate the individual samples, showing that each individually prepared sample gives a similar result. Middle: Again the fitted periodicity, the colouring is the same as in the left panel, indicating the cell number. The vertical-axis shows the length of the measured filament. The periodicity does not show a clear correlation between filament length and as could be expected, with an increased length of the filaments the spread in fitted periodicity decreases, as the fitting becomes more precise. Right: Histogram of the fitted period, with the length of the filament taken to weight. The red line is the mean of the fitted Gauss (74.67 nm, STD= 2.09). The mean of the length-weighted period is 74.87. (F) Similar to (E), but this time from three samples (plus one cell from a fourth sample), a total of 38 cells have been imaged with STED microscopy to study the periodicity of CEP68. As for rootletin, the filaments show a large spread in the total length, and lengths up to 1.34 µm have been measured. As for rootletin, many line profiles (66 of the 208) were difficult to fit a sine-function to. Results of 142 line-profiles with a total length of 73.54 nm (~984 periods) are shown. In the histogram, the red line is the mean of the fitted Gauss (74.73 nm, STD= 2.57) and the mean period of the length-weighted data is 75.52 nm.

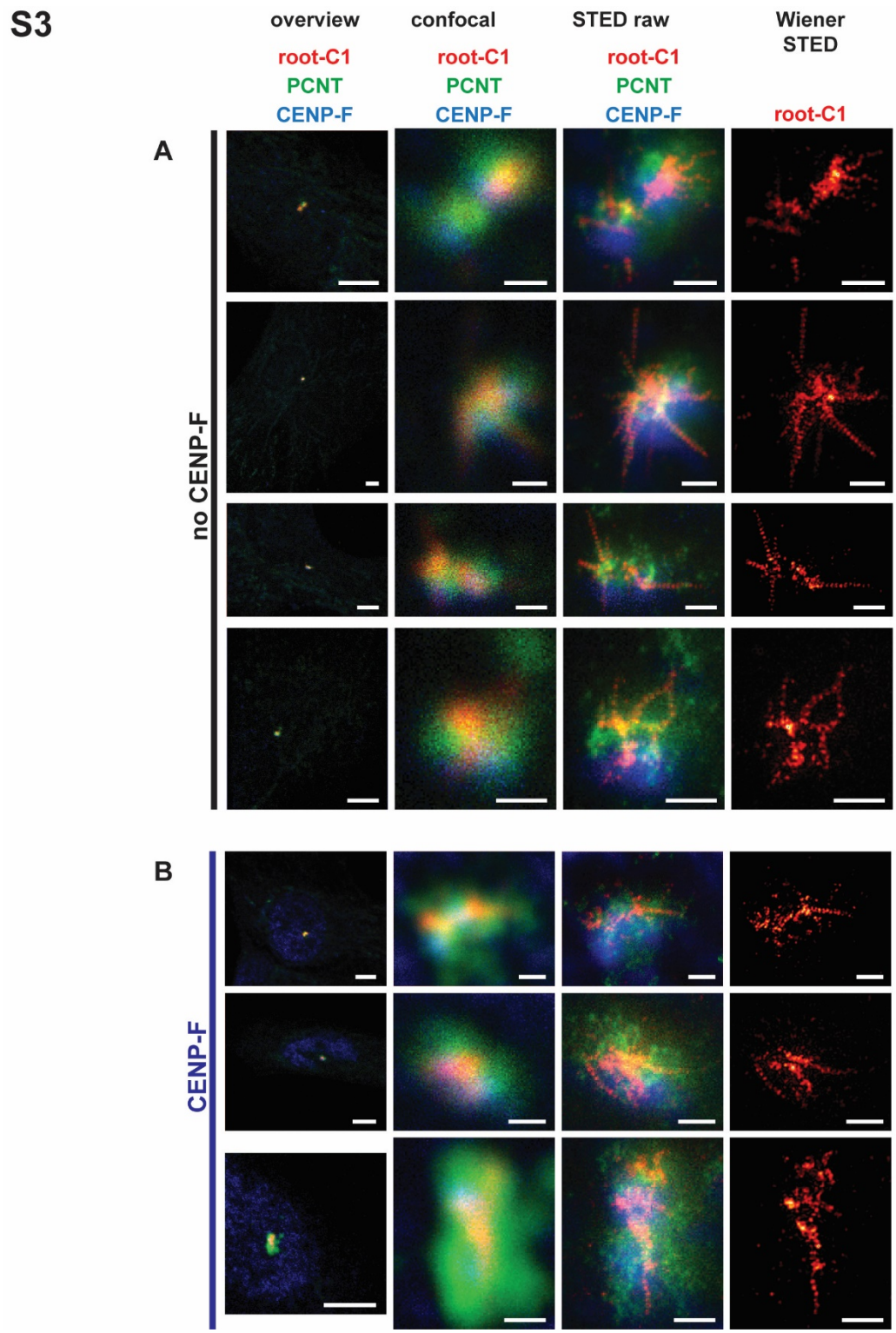

Supplemental Fig. 3. Analysis of the cell cycle dependency of rootletin filaments (root-C1). (A, B) We stained for the cell cycle marker CENP-F which does not stain the nucleus in G1 and S phase cells but decorates the nuclear envelope and associates with kinetochores starting in G2. Cells that lack CENP-F (A), as well as cells that show nuclear CENP-F signal (B) both show similar structures to those shown in Fig. 1, and therefore our analysis reflects the G1, S and early G2 organisation of the centrosome linker.

S4

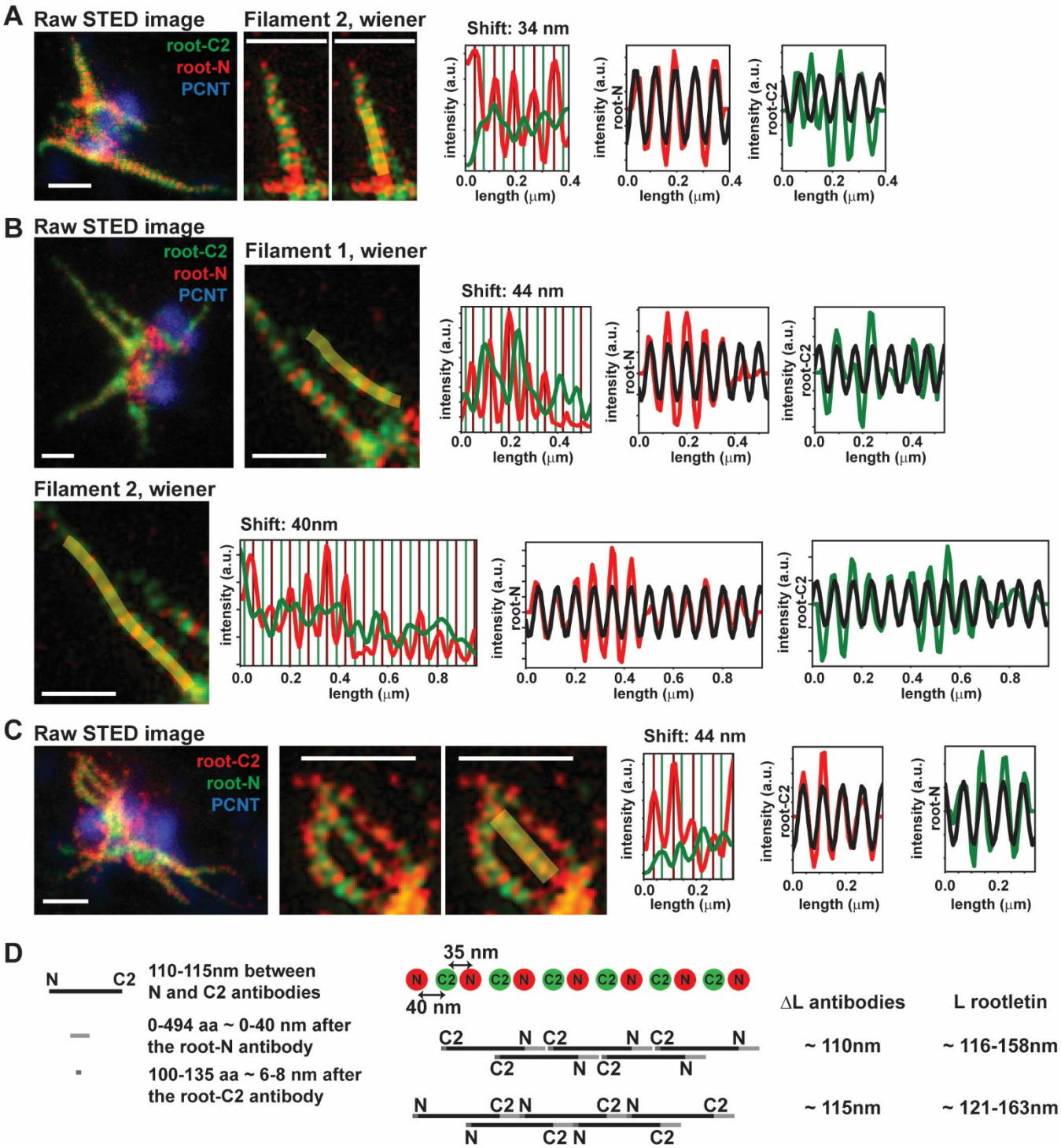

Supplemental Fig. 4. Rootletin N-terminus and C-terminus localisation along the fibre. (A) Of the same cell as Fig. 3A, the raw STED image is shown where the N- and C-terminus staining are through root-N (red) and root-C2 (green) antibodies, respectively. Through confocal microscopy, also PCNT (blue) was imaged. Now another filament in another direction is shown. The location of root-C2 is ~34 nm more outward than root-N. (B) Another cell (raw data), and the line profiles of two individual filaments are shown (Wiener deconvolved).

According to the sine-fit to each of the proteins, the location of root-C2 is ~44 nm and ~40 nm more outward than root-N for each of these filaments. (C) 'Reversed' staining. Where in A) and B) root-N is attached to the kk114L dye and root-C2 to the star580 dye, this cell has the kk114L dye to the root-C2 antibody and the star580 dye to the root-N antibody. Again a similar result is obtained (44 nm) for the localisation of C2 compared to N. (D) From the localisations of the root-C2 and root-N antibodies, the length of rootletin can be estimated. By just connecting the two fluorophores the rootletin length between the antibodies is estimated to be between 110 and 115 nm. However, the antibodies do not need to be at the extremes of rootletin, thus this estimate is a lower length estimate. For root-N we have a binding uncertainty of 494 amino acids. For root-C2 we have a binding uncertainty of only 35 amino acids, but we also know that it is at least 100 amino acids away from the protein end. Interpolating the length per amino acid, rootletin thus has an estimated length of 116-158 nm or 121-163 nm, depending on the overlap, as drawn. All scale bars 500 nm.

S5

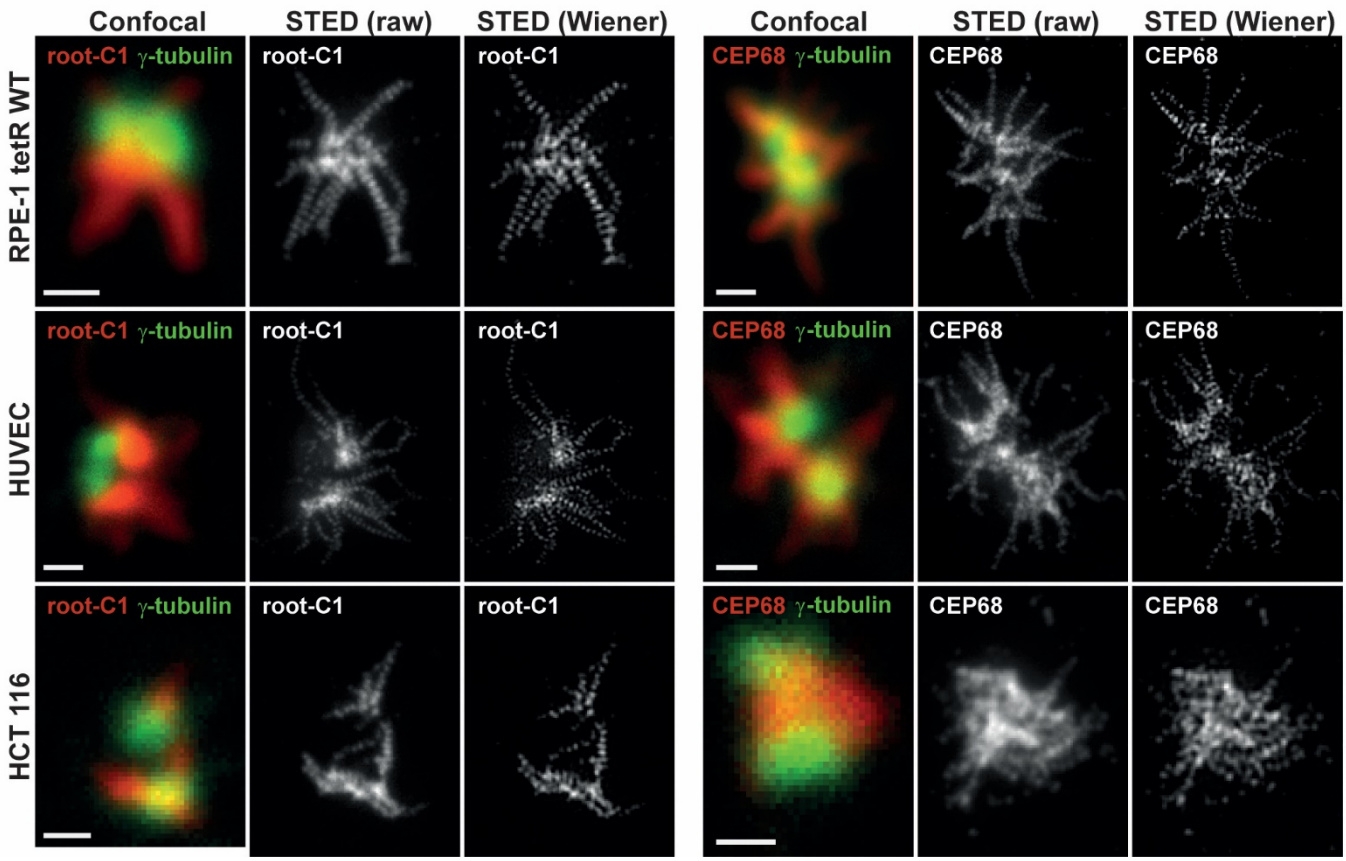

Supplemental Fig. 5. Rootletin network in RPE-1 tetR WT, HUVEC and HCT116 cells. Rootletin and CEP68 as analysed by STED using C-terminal rootletin (root-C1) antibody or an antibody directed against CEP68. RPE-1, primary HUVEC (passage 4) and HCT116 cells were analysed. To show the effect of the background subtraction and the Wiener filter, as described in materials and methods, the raw and filtered STED images are both shown. Scale bars, 500 nm.

S6

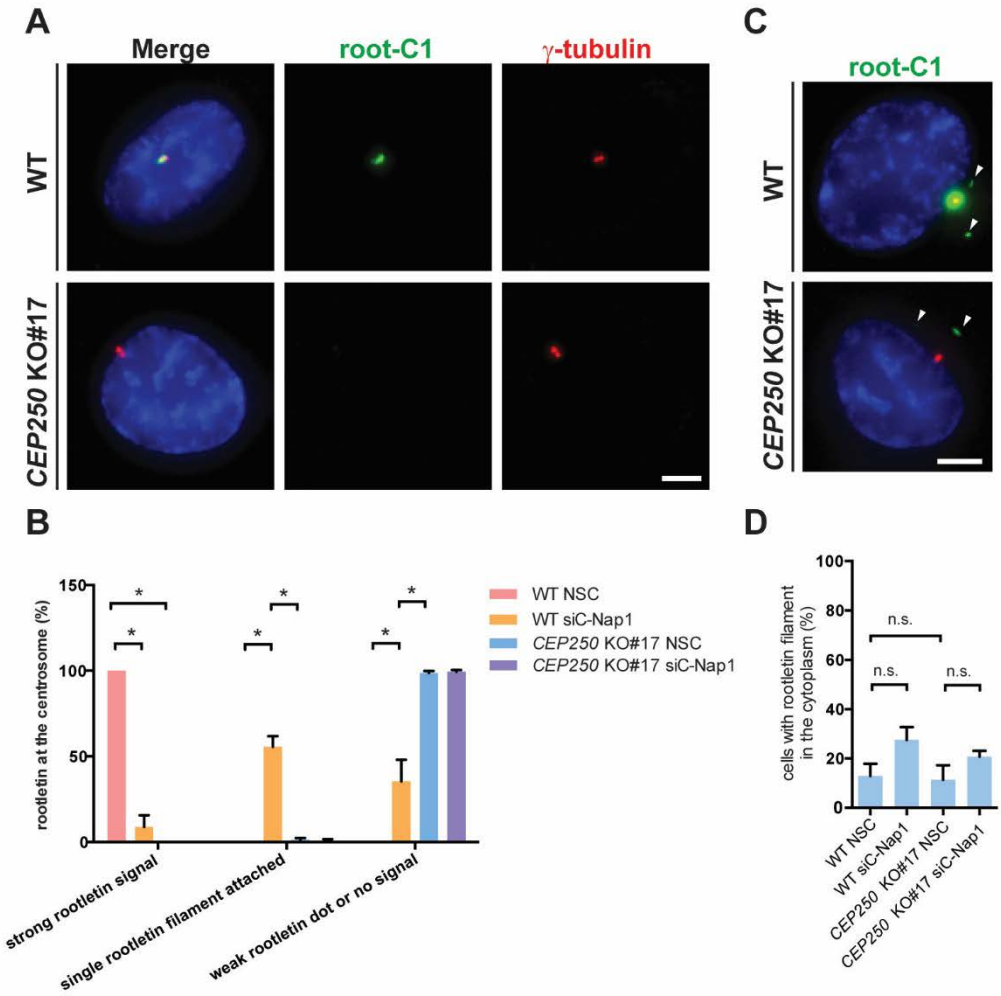

Supplemental Fig. 6. (A) Absence of rootletin (root-C1) from centrioles in CEP250 KO cells. RPE-1 tetR WT NSC, WT siC-Nap1, CEP250 KO and CEP250 KO siC-Nap1 cells were analysed by indirect immunofluorescence (IF) for rootletin phenotype with γ-tubulin marked centrioles. Shown are examples of RPE-1 tetR WT and CEP250 KO cells. (B) Quantification of (A). n = 3, N ≥ 50, mean and SD are shown. * Difference is significant in t-test. (C) Cytoplasmic rootletin filaments were found to a similar degree in WT NSC, WT siC-Nap1, CEP250 KO NSC, CEP250 KO siC-Nap1 RPE-1 cells. This indicates that rootletin filaments can form in the cytoplasm without C-Nap1. (D) Quantification of cells with cytoplasmic rootletin filaments from (C). n = 3, N ≥ 50, mean and SD are shown. (A, C) Scale bars, 5 µm. N.s.: no significant difference was found in t-test.

S7

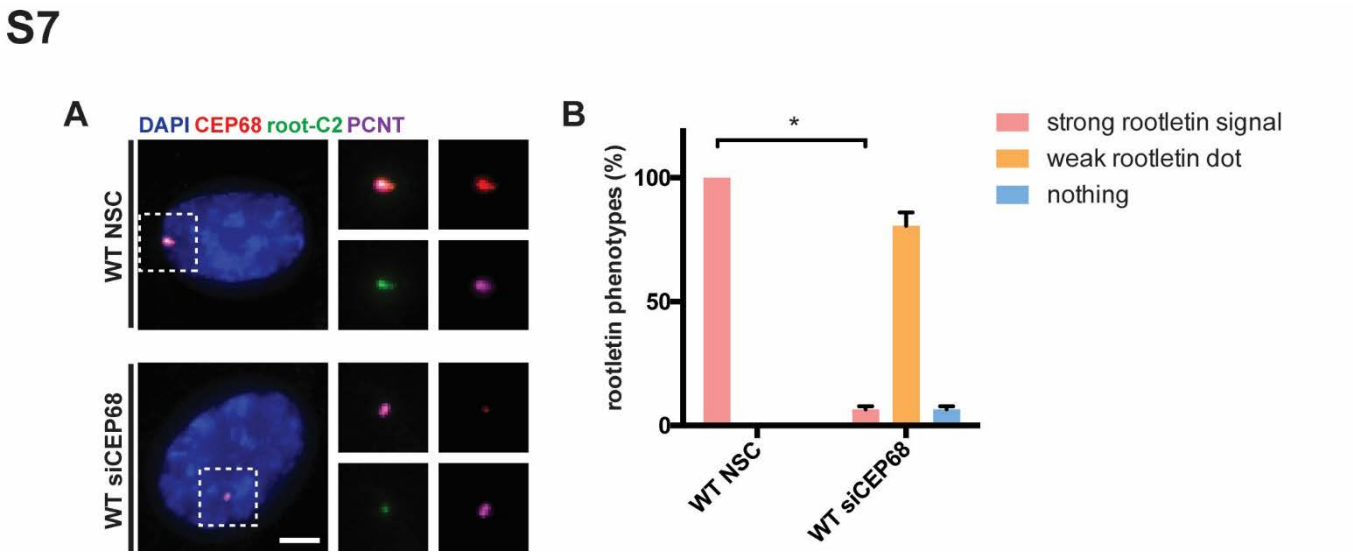

Supplemental Fig. 7. siRNA depletion of CEP68 reduces most rootletin filaments from centrosomes. Cells were analysed by indirect immunofluorescence with the indicated antibodies. (*A*) siRNA depletion of CEP68 in RPE-1 cells. Scale bar, 5 µm. (*B*) Quantification of (*A*). n = 3, N ≥ 50, mean and SD are shown. * Difference is significant in t-test.

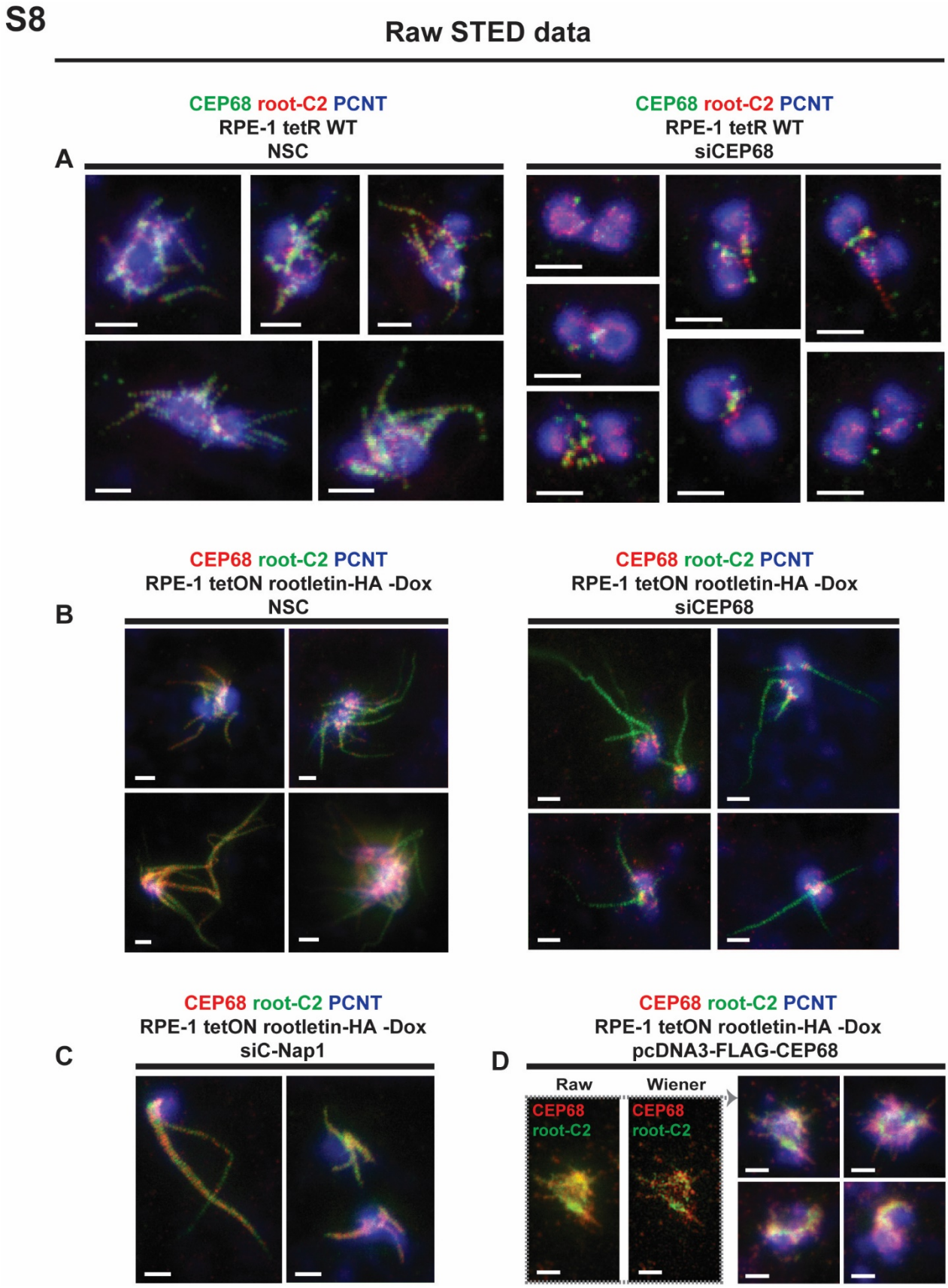

Supplemental Fig. 8. More examples of the STED analysis of centriolar CEP68/rootletin structures under different conditions. PCNT was used as a marker for centrioles. All images

are raw STED images, unless specified otherwise. (*A*) The non-specific control (NSC) versus the siRNA depleted CEP68 cells. (*B*) The non-specific control (NSC) versus the siRNA depleted CEP68 cells in the presence of mildly overexpressed *CROCC* (rootletin) (-Dox). (*C*) The siRNA depletion of C-Nap1 in cells that mildly overexpress *CROCC* (rootletin) in absence of Dox. (*D*) In the presence of both overexpressed *CROCC* (rootletin) as well as overexpressed *CEP68*, the filament structure is not recognisable anymore and large dense structures are being formed. To the left the Wiener filtered example of one of those cells is shown to illustrate that we cannot distinguish filamentous structures anymore. All scale bars 500 nm.

S9

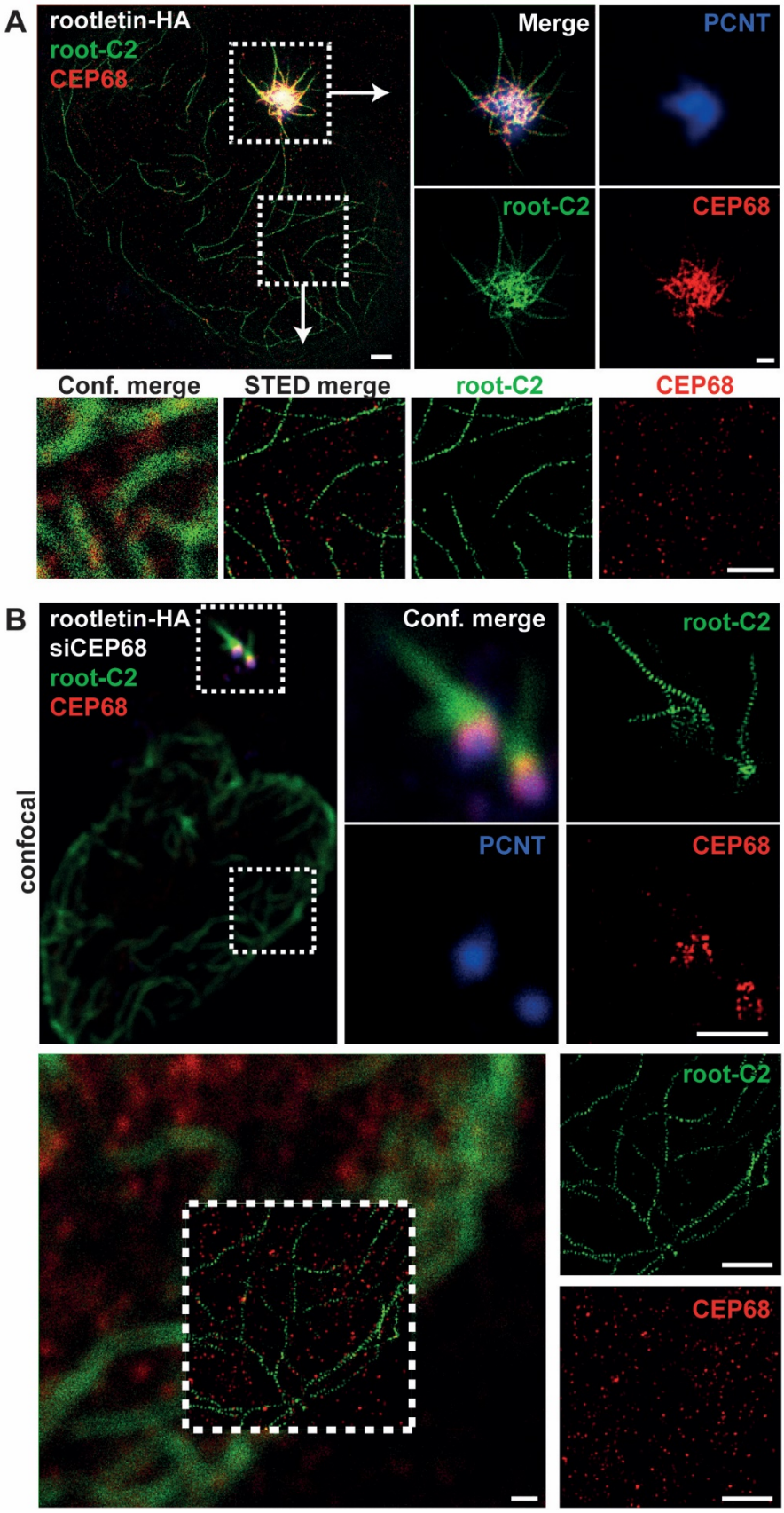

Supplemental Fig. 9. Dual colour STED analysis of CEP68 and rootletin organisation under mild overexpression of *CROCC* (rootletin) in RPE-1 tetR cells (A) CEP68 mostly assembles

onto rootletin fibres at the centrosome. In this cell, free CEP68 did not specifically co-localise with thin rootletin fibres (root-C2, bottom). (B) siRNA depletion of CEP68 in *CROCC* (rootletin) overexpressing cells did significantly decrease the number of rootletin fibres at the centrosome. Cells contain mostly thin rootletin fibres (root-C2) outside the centrosome region that were not decorated by CEP68. Scale bars 500 nm.

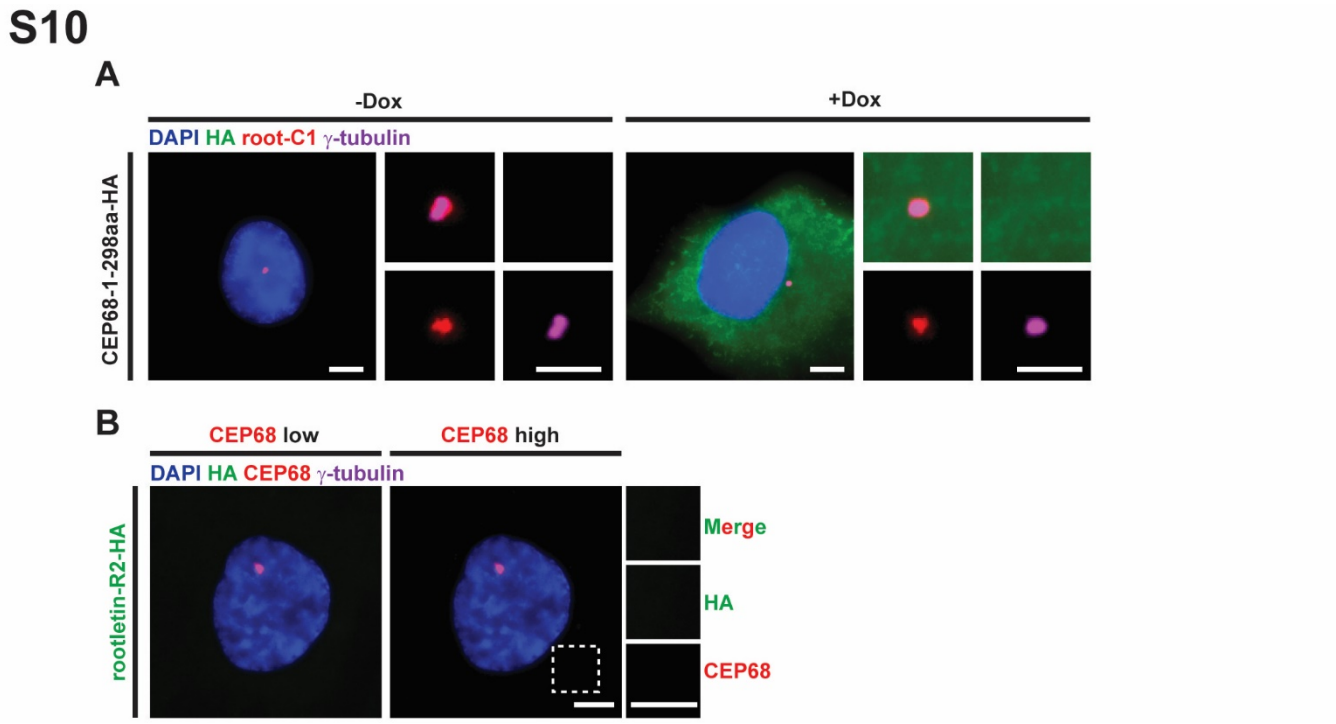

Supplemental Fig. 10. (*A*) N-terminal of CEP68 does not bind to centrosomes marked by γ-tubulin. (*B*) R2 fragment of rootletin was not detectable by IF in RPE-1 cells. (*A*, *B*) Scale bars, 5 µm.

S11

Raw STED data figure 1

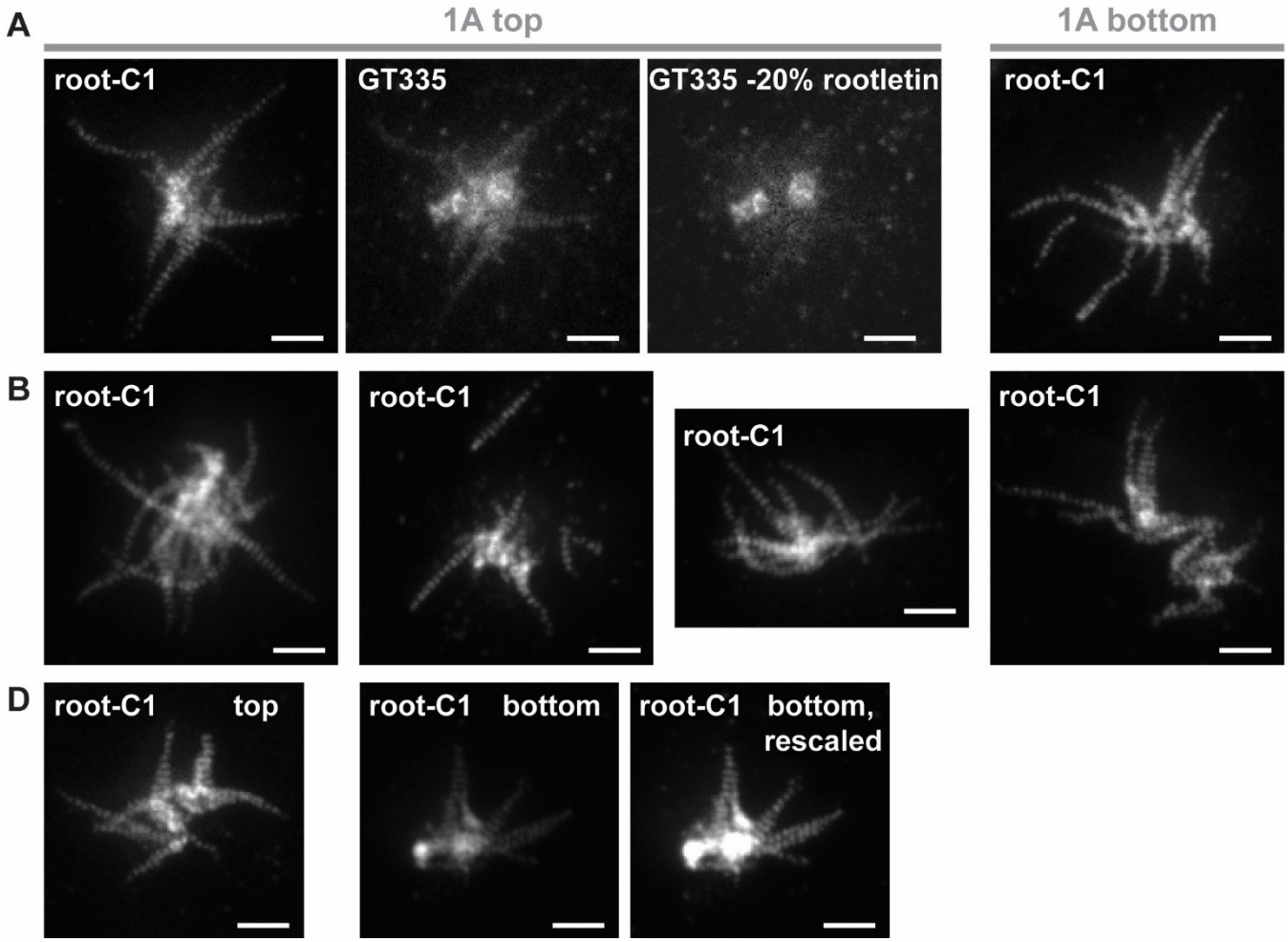

S11

Raw STED data figure 2

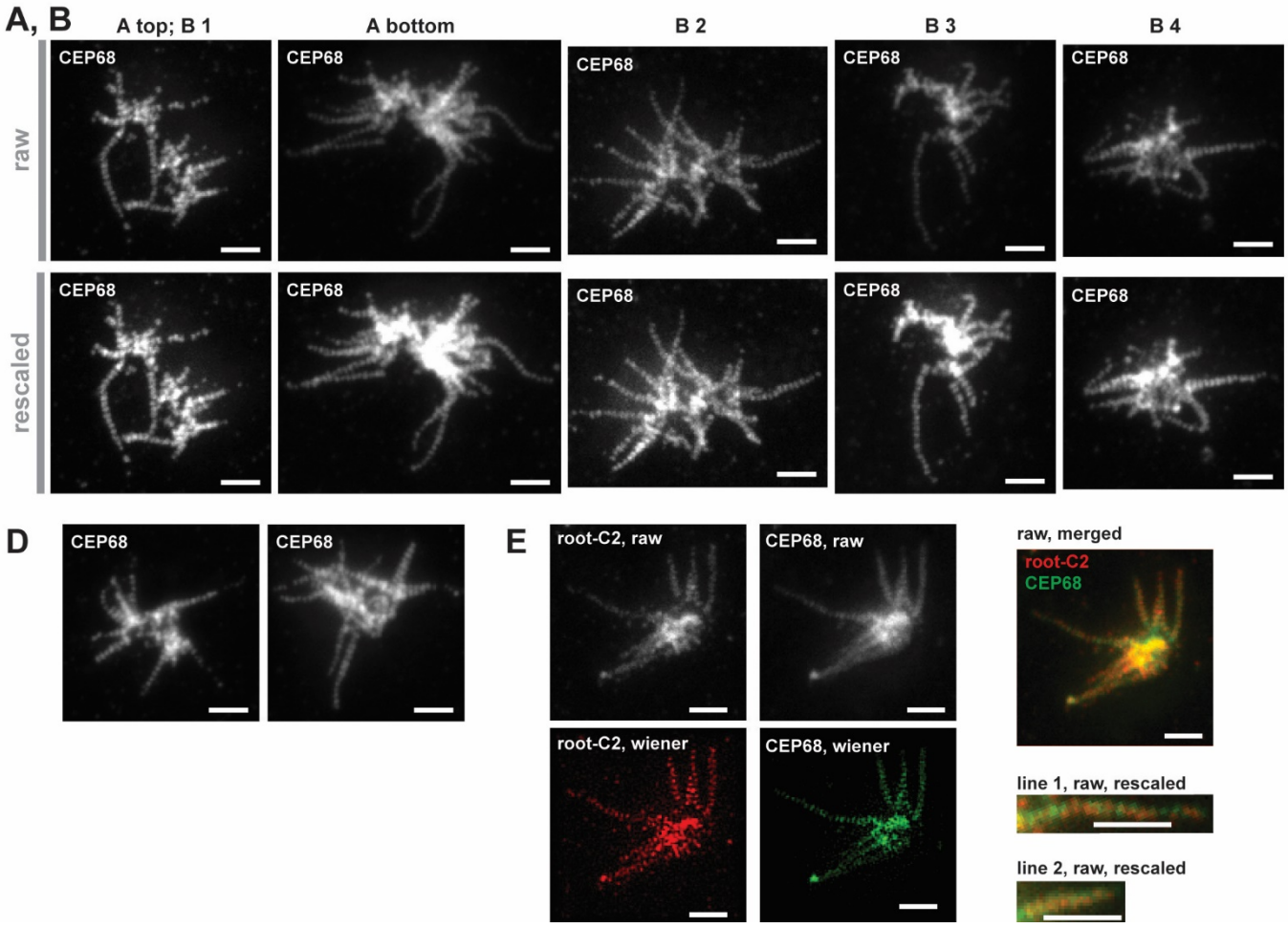

S11

Raw STED data figure 3 and S4

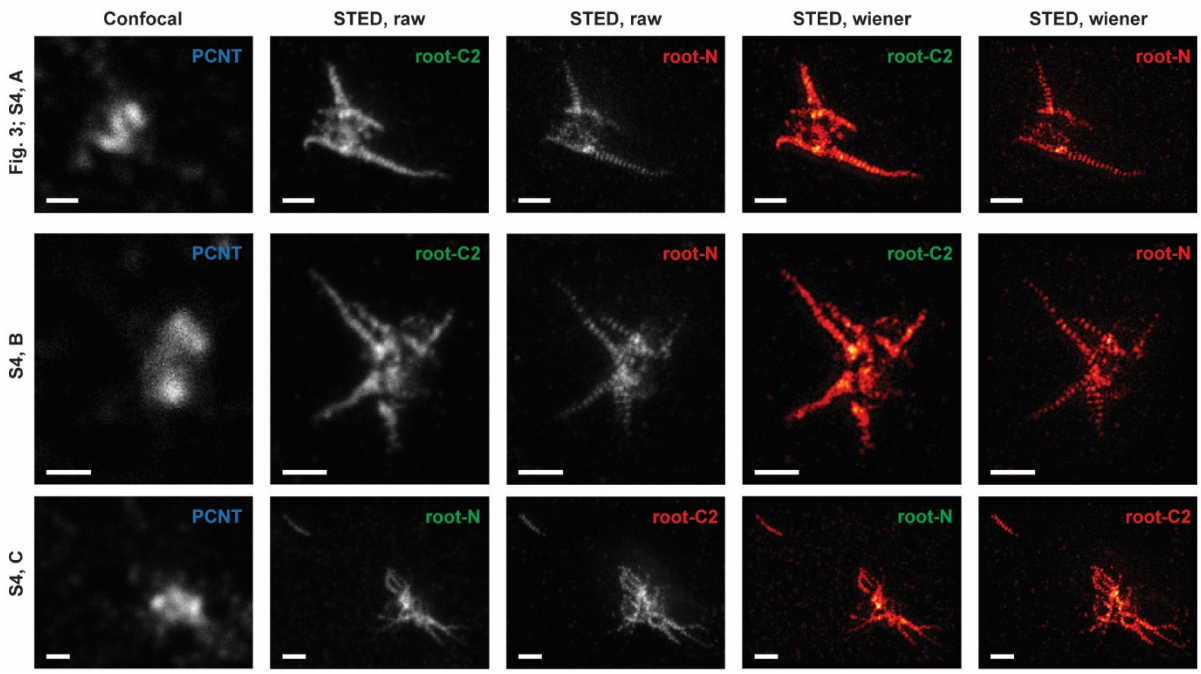

S11

Raw STED data figure 4

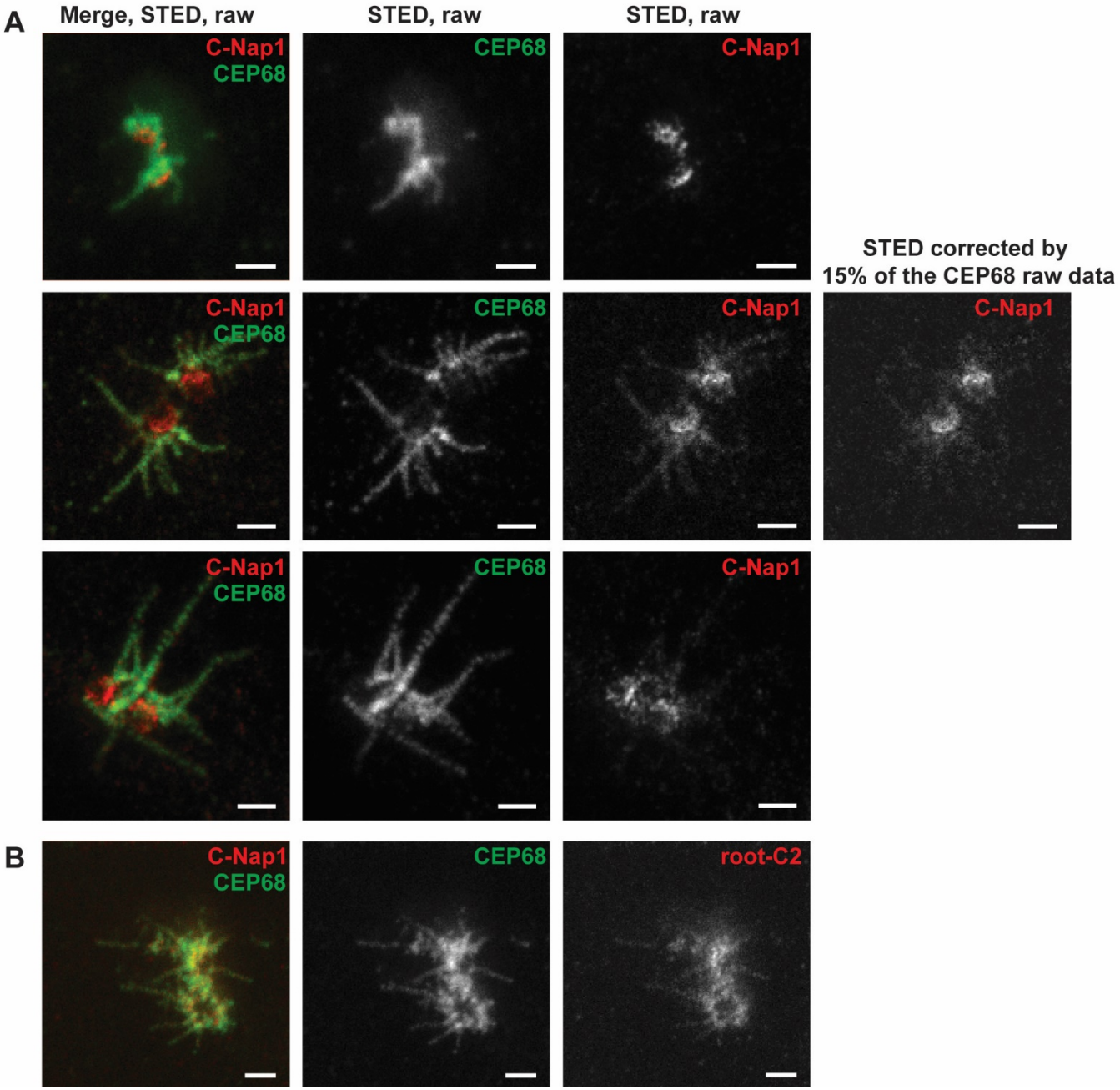

S11

Raw STED data figure 5

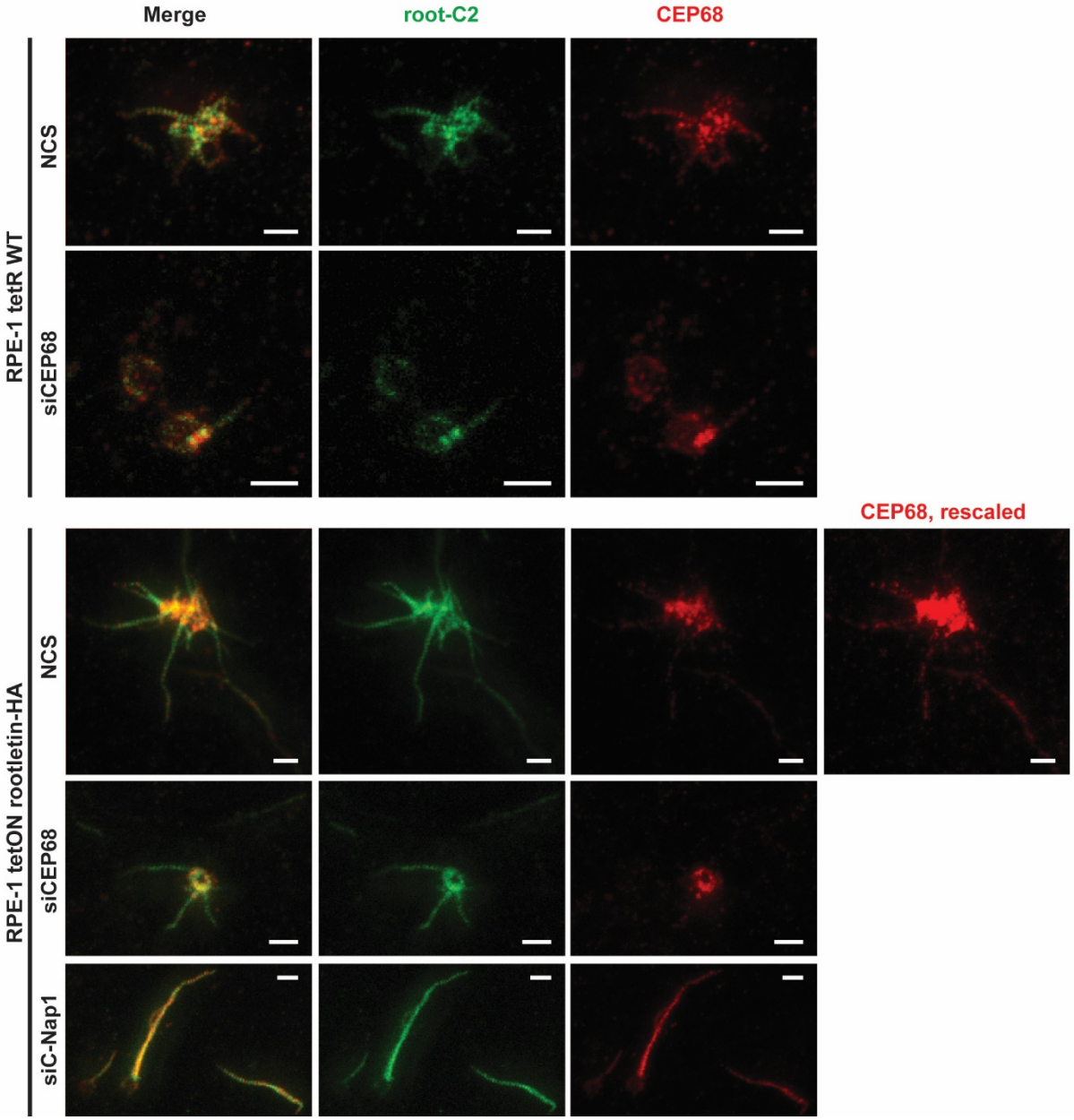

S11 Raw STED data figure 6

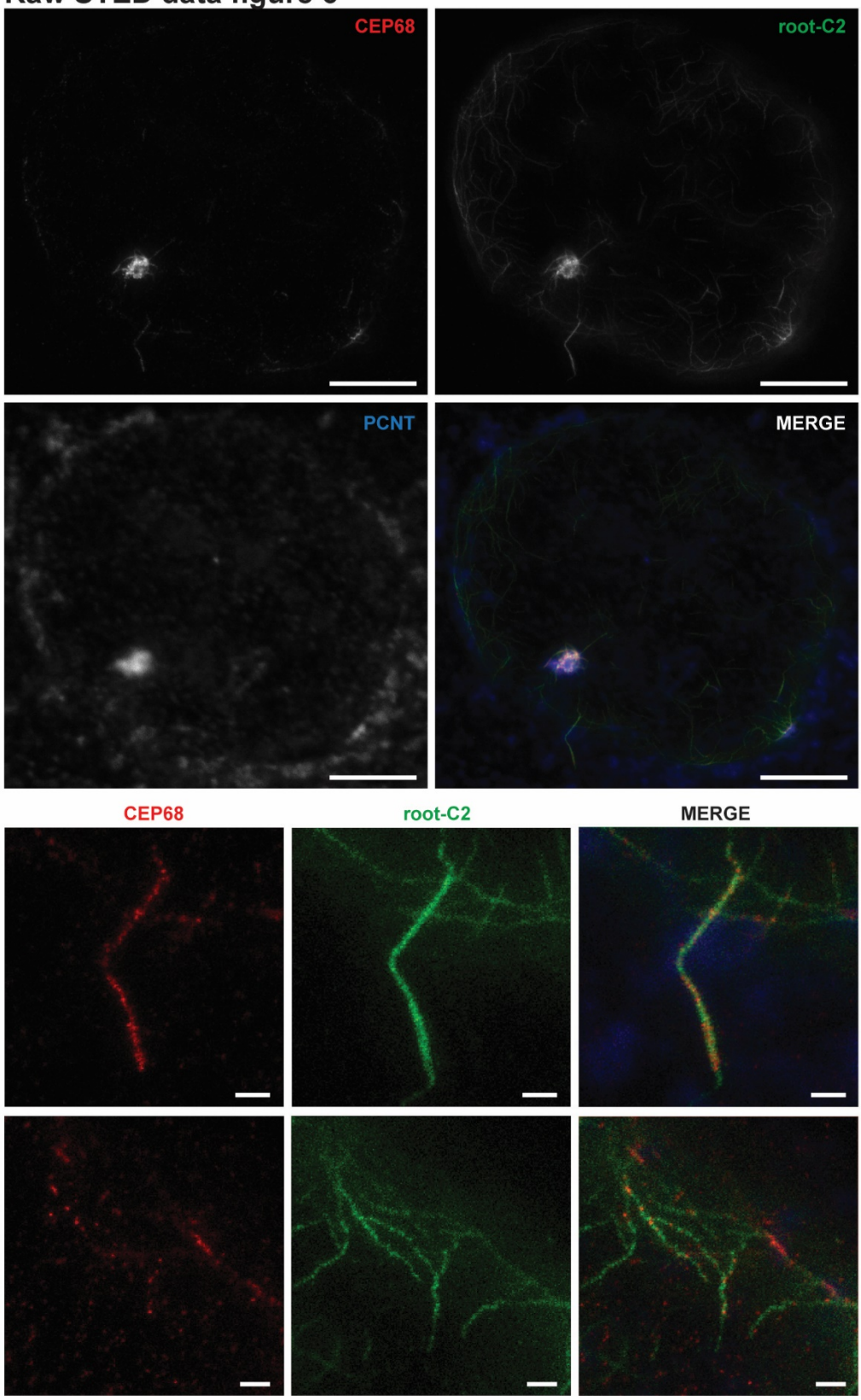

Supplemental Fig. 11. The figures in the main text are, unless specified otherwise, Wiener deconvolved images. All raw STED images are shown here. As only part of the data could be shown in the paper, representative images are chosen to illustrate the typical structure.

S12

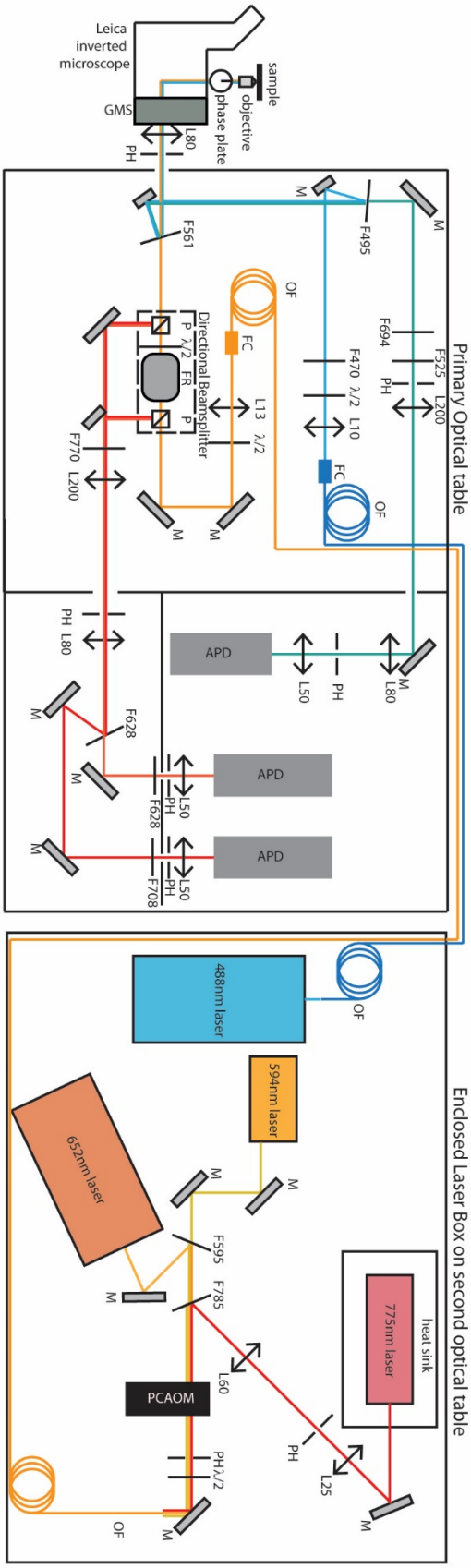

Supplemental Fig. 12. Home-built STED microscope as used for all data, except Fig. 3A, B, Fig 4A lower two panels, Fig. 5B siCEP68, Fig. S3, Fig. S4 A, B, C and the corresponding

figures in S11. For these figure a commercial Abberior Instruments 775 STED was used. APD = avalanche photodiode; F = filter of types:Z470/10X 61138; Semrock 496/LP BrightLine HC Langpass-Filter; Semrock 525/50 nm BrightLine® single-band bandpass filter; Semrock 561 nm laser BrightLine® single-edge super-resolution laser dichroic beamsplitter; Chroma filter ET bandpass 595/50 M-2P; Semrock 628/32 nm BrightLine® single-band bandpass filter; Semrock 694 nm blocking edge BrightLine® short-pass filter; Semrock 708/75 nm BrightLine® single-band bandpass filter; Semrock 770 nm blocking edge BrightLine® multiphoton short-pass emission filter; Semrock RazorEdge short wave pass filter 785nm, #SP01-785RU-25 ; FC = fibre coupler; FR = leysop Faraday Rotator; GMS = galvano-meter scanners; λ/2 = λ /2 plate; L= lens with focal lengths in mm; M = mirror; OF = optical fibre; P = polarizing beamsplitter cubes; PCAOM = polychromatic acousto-optical modulator; PH = Pin hole.

Supplemental Table

Supplemental Table 1. The number of cells measured for each STED experiment.; in total 901 cells were measured using STED microscopy.

Cell Line	STED		Confocal	Cell #
RPE-1 tetR	CEP68		± γ-tubulin	108
RPE-1 tetR	CEP68	C-Nap1	±PCNT	113
RPE-1 tetR	CEP68	root-C2	-	42
RPE-1 tetR	C-NAP1	± PCNT	cep164	71
RPE-1 tetR	root-N	root-C2	± C-Nap1	101
RPE-1 tetR	root-C1	GT335		13
RPE-1 tetR	root-C1		± γ-tubulin	69
RPE-1 tetR	root-C1	PCNT	CENPF	15
RPE-1 tetON rootletin-HA ±DOX	root-C1		HA	21
RPE-1 tetON rootletin-HA	root-C2	CEP68	PCNT	16
RPE-1 tetON rootletin-HA NSC	root-C2	CEP68	PCNT	13
RPE-1 tetON rootletin-HA + siCEP68	root-C2	CEP68	PCNT	10
RPE-1 tetON rootletin-HA + pcDNA3-FLAG	root-C2	CEP68	PCNT	13
RPE-1 tetON rootletin-HA + pcDNA3-FLAG-CEP68	root-C2	CEP68	PCNT	7
RPE-1 tetON rootletin-HA +siC-Nap1	root-C2	CEP68	PCNT	24
RPE-1 tetON CEP68-HA ±DOX	root-C2	CEP68	PCNT	12
RPE-1 tetON CEP68-HA ±DOX	root-C1		HA	22
RPE-1 tetR + siCEP68	root-C2	CEP68	PCNT	45
RPE-1 tetR + siCEP68	root-C2		PCNT	14
RPE-1 tetR + NSC	root-C2	± CEP68	PCNT	32
HCT	root-C1		γ-tubulin	72
HCT	CEP68		γ-tubulin	23
HUVEC	root-C1		γ-tubulin	22
HUVEC	CEP68		γ-tubulin	23

Supplemental References

1. Heilemann M*, et al.* (2008) Subdiffraction-resolution fluorescence imaging with conventional fluorescent probes. *Angew Chem Int Ed Engl* 47(33):6172-6176.
2. Venkataramani V, Herrmannsdorfer F, Heilemann M, & Kuner T (2016) SuReSim: simulating localization microscopy experiments from ground truth models. *Nat Methods* 13(4):319-321.
3. Edelstein AD*, et al.* (2014) Advanced methods of microscope control using muManager software. *J Biol Methods* 1(2).
4. Wolter S*, et al.* (2012) rapidSTORM: accurate, fast open-source software for localization microscopy. *Nat Methods* 9(11):1040-1041.
5. El Beheiry M & Dahan M (2013) ViSP: representing single-particle localizations in three dimensions. *Nat Methods* 10(8):689-690.
6. Panic M, Hata S, Neuner A, & Schiebel E (2015) The centrosomal linker and microtubules provide dual levels of spatial coordination of centrosomes. *PLoS Genet* 11(5):e1005243.
7. Graser S, Stierhof YD, & Nigg EA (2007) Cep68 and Cep215 (Cdk5rap2) are required for centrosome cohesion. *J Cell Sci* 120(Pt 24):4321-4331.
8. Fava LL*, et al.* (2017) The PIDDosome activates p53 in response to supernumerary centrosomes. *Genes Dev* 31(1):34-45.
9. Wolff A*, et al.* (1992) Distribution of glutamylated alpha and beta-tubulin in mouse tissues using a specific monoclonal antibody, GT335. *Eur J Cell Biol* 59(2):425-432.